

Dissipatively dressed quasiparticles in boundary driven integrable spin chains

Vladislav Popkov,^{1, 2, 3} Xin Zhang,^{4, 3} Carlo Presilla,^{5, 6} and Tomaž Prosen^{1, 7}

¹*Faculty of Mathematics and Physics, University of Ljubljana, Jadranska 19, SI-1000 Ljubljana, Slovenia*

²*Department of Physics, University of Wuppertal, Gaussstraße 20, 42119 Wuppertal, Germany*

³*These two authors contributed equally to this work*

⁴*Beijing National Laboratory for Condensed Matter Physics,*

Institute of Physics, Chinese Academy of Sciences, Beijing 100190, China

⁵*Dipartimento di Matematica, Università di Roma La Sapienza, Piazzale Aldo Moro 5, Roma 00185, Italy*

⁶*Istituto Nazionale di Fisica Nucleare, Sezione di Roma 1, Roma 00185, Italy*

⁷*Institute of Mathematics, Physics and Mechanics, Jadranska 19, SI-1000 Ljubljana, Slovenia*

The nonequilibrium steady state (NESS) of integrable spin chains experiencing strong boundary dissipation is accounted by introducing quasiparticles with a renormalized—dissipatively dressed—dispersion relation. This allows us to evaluate the spectrum of the NESS in terms of the Bethe ansatz equations for a related coherent system which has the same set of eigenstates, the so-called dissipation-projected Hamiltonian. We find explicit analytic expressions for the dressed energies of the XXX and XXZ models with effective, i.e., induced by the dissipation, diagonal boundary fields, which are U(1) invariant, as well as the XXZ and XYZ models with effective non-diagonal boundary fields. In all cases, the dissipative dressing generates an extra singularity in the dispersion relation, substantially altering the NESS spectrum with respect to the spectrum of the corresponding coherent model.

I. INTRODUCTION

The notion of quasiparticles is a fundamental concept in regular many-body systems irrespectively on whether they are integrable or not. Examples of quasiparticles are phonons in crystals and magnons in magnetic materials. In integrable continuous theories with nonlinearities (e.g. in Korteweg de Vries or sine-Gordon models), stable quasiparticles are solitons, or solitary waves which are spatially localized: after a collision they retain their original velocities and shapes, the net result of the scattering being just a shifting of their world lines. Quasiparticles of integrable quantum interacting manybody systems on a lattice also possess special properties with regard of their multiple scattering: the multiple quasiparticle collision can be factorized in terms of two-body scattering matrix. Every eigenstate in an integrable quantum system can be viewed as consisting of quasiparticles. Most prominently, the eigenenergy of any eigenstate is obtainable by summing individual energies of all quasiparticles it contains $E_\alpha = \sum_j \epsilon(u_{j,\alpha})$ where $u_{j,\alpha}$ are set of admissible rapidities and $\epsilon(u)$ is a dispersion relation. The dispersion relation $\epsilon(u)$ is a fundamental property of quasiparticles, and it is very robust, e.g. the dispersion does not depend on boundary conditions, temperature, system size etc.

The purpose of our communication is to establish a relation between two fundamental quantities from seemingly very different fields: the spectrum E_α of a coherent (closed) integrable many-body system, from one side, and the spectrum λ_α of a non-equilibrium steady state of the “same” open quantum system in contact with locally acting dissipative bath, from another side. In more details, we will demonstrate that under a proper choice of the dissipation, there exists a one-to one correspondence between the two spectra, namely that $\log \lambda_\alpha = \sum_j \tilde{\epsilon}(u_{j,\alpha})$

where $u_{j,\alpha}$ is exactly the same sets of admissible rapidities, constituting the spectrum of a coherent system $E_\alpha = \sum_j \epsilon(u_{j,\alpha})$, and $\tilde{\epsilon}(u)$ is a renormalized dispersion (we refer to it as *dissipatively dressed dispersion relation*). An existence of a renormalized dispersion relation relating coherent (unitary) and strongly incoherent (dissipative) systems seems rather counterintuitive; however its general validity lies beyond what we are currently able to prove.

We compare an equilibrium Gibbs state ρ_{Gibbs} of a quantum integrable many-body system, from one side, and a nonequilibrium steady state ρ_{NESS} of “almost the same” system, with a part of degrees of freedom coupled to a dissipative bath, from the other side. The Gibbs state is

$$\rho_{\text{Gibbs}} = \frac{1}{Z} \sum_{\alpha} e^{-\beta E_{\alpha}} |\alpha\rangle \langle \alpha|, \quad (1)$$

$$E_{\alpha} = \sum_j \epsilon(u_{j,\alpha}),$$

where $\epsilon(u)$ is the dispersion relation of the quasiparticles, and $u_{j,\alpha}$ are the admissible rapidities, obtained via the quantization conditions, namely, a set of Bethe ansatz equations (BAE) obtainable by different methods [1–5]. The type of quasiparticles and their number depend on the model and the intrinsic quantum numbers characterizing the microstates $\{|\alpha\rangle\}$.

In the dissipative setup, we consider a “similar” quantum system, with boundary degrees of freedom coupled to a dissipative bath, described via a Lindblad Master equation. This leads to a nonunitary dynamics of a reduced density matrix $\rho(t)$, which relaxes to a (unique) nonequilibrium steady state (NESS), $\lim_{t \rightarrow \infty} \rho(t) = \rho_{\text{NESS}}$. In general, there is no reason to expect any close relation between the Gibbs state (1) and the nonequilibrium NESS.

The purpose of this communication is to show, that under certain conditions, (A) the NESS has the same set of eigenstates $|\alpha\rangle$ as (1), i.e.

$$[\rho_{\text{NESS}}, \rho_{\text{Gibbs}}] = 0, \quad (2)$$

and, (B) the effective energies \tilde{E}_α are described by exactly the same quasiparticle content as E_α , i.e. are given by the sum of the same set of quasiparticles as in (1), but with renormalized—“dissipatively dressed”—dispersion relation $\epsilon(u) \rightarrow \tilde{\epsilon}(u)$,

$$\rho_{\text{NESS}} = \frac{1}{\tilde{Z}} \sum_{\alpha} e^{-\tilde{E}_\alpha} |\alpha\rangle \langle \alpha|, \quad (3)$$

$$\tilde{E}_\alpha = \sum_j \tilde{\epsilon}(u_{j,\alpha}). \quad (4)$$

The relation (4) is very surprising: it suggests that the notion of Bethe quasiparticles (a intrinsic property of a coherent integrable system) can, under certain conditions, be preserved under dissipation, at least with respect to its steady state (NESS).

The following sections serve to explain the relation between coherent and dissipation-affected quantum systems in detail.

We note that this is a companion paper expanding on a recent exact result [6], here including heuristic and numerical evidence in a broader family of integrable models and dissipation setups.

II. INTEGRABLE SPIN CHAINS WITH BOUNDARY FIELDS AND BOUNDARY-DRIVEN SPIN CHAINS

Our coherent system is a general open spin $\frac{1}{2}$ chain described by nearest neighbour Heisenberg Hamiltonian with general boundary fields $h_1 = \vec{h}_1 \cdot \vec{\sigma}_1$ and $h_N = \vec{h}_N \cdot \vec{\sigma}_N$,

$$H = H_{\text{bulk}} + h_1 + h_N \quad (5)$$

$$H_{\text{bulk}} = \sum_{n=1}^{N-1} \vec{\sigma}_n \hat{J} \vec{\sigma}_{n+1}, \quad \hat{J} = \text{diag}(J_x, J_y, J_z). \quad (6)$$

It is known, see [7, 8], that the above system is integrable for any choice of $J_x, J_y, J_z, \vec{h}_1, \vec{h}_N$. More popular examples of XXZ and XXX model result from reductions $J_x = J_y$ and $J_x = J_y = J_z$. As such, any eigenstate of (5) has a quasiparticle content, with admissible values of the rapidities in (1), given by the respective Bethe Ansatz equations [8]. Later on, the boundary fields will be specified.

On the dissipative side, our scenario is as follows: we have a spin chain of $N + 2$ sites (note that there are two extra sites w.r.t. the coherent system above), described by the Hamiltonian $H = \sum_{n=0}^N \vec{\sigma}_n \hat{J} \vec{\sigma}_{n+1}$ (the

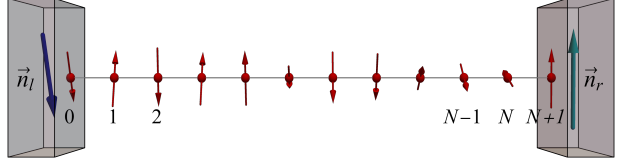


Fig. 1. Schematic picture of the dissipative setup. The boundary spins are fixed by dissipation, while the internal spins follow effective dynamics (13), consisting of fast coherent dynamics (5) and slow relaxation dynamics (17) towards the NESS.

same Hamiltonian as in (6) with 2 sites added), in which the edge spins, those at positions $n = 0$ and $n = N+1$ are projected on pure qubit states ρ_l, ρ_r respectively, by coupling to a dissipative Lindblad bath. Schematic picture is given in Fig.1.

The time evolution of the reduced density matrix is described by the Lindblad Master equation

$$\frac{\partial \rho(\Gamma, t)}{\partial t} = -i[H, \rho] + \Gamma (\mathcal{D}_{L_1}[\rho] + \mathcal{D}_{L_2}[\rho]) \quad (7)$$

$$\mathcal{D}_L[\rho] = L \rho L^\dagger - \frac{1}{2} (L^\dagger L \rho + \rho L^\dagger L). \quad (8)$$

The Lindblad operators can be conveniently chosen in a form $L_1 = |\psi_l\rangle \langle \psi_l|^\perp \otimes I^{\otimes N+1}$, $L_2 = I^{\otimes N+1} \otimes |\psi_r\rangle \langle \psi_r|^\perp$, where $\langle \psi^\perp | \psi \rangle = 0$. Indeed the Lindblad dissipators \mathcal{D}_{L_1} and \mathcal{D}_{L_2} will then promote the relaxation of edge spins to targeted pure states $|\psi_{l,r}\rangle$, with typical relaxation time $\tau_{\text{boundary}} = O(1/\Gamma)$. We will consider the case when τ_{boundary} is much smaller than a typical time needed for the bulk relaxation $\tau_{\text{boundary}} \ll \tau_{\text{bulk}}$, the so-called quantum Zeno (QZ) regime. Note that Γ need not be necessarily very large to reach QZ; e.g. for XXX bulk Hamiltonian $J_x = J_y = J_z$ the effective $\Gamma = O(N^{-1})$ as shown in [9].

The quantum Zeno regime with arbitrary Γ can be realized by a protocol of repeated interactions. In this protocol, the edge spin is repeatedly brought in contact with a freshly polarized magnet, see e.g.[10]. Alternatively, an instantaneous projection of a single qubit can be achieved by applying of a so-called reset gate [11]: the gate simply resets a qubit state to a desired qubit state at each application. In Appendix A we give a derivation of (7) from a qubit circuit protocol.

The fast relaxation of the edge spins in QZ regime constrains the reduced density matrix of (7) to an approximately factorized form [12] $\rho(\Gamma, t) = \rho_l \otimes \rho(\Gamma, t) \otimes \rho_r + O(1/\Gamma)$ for $t \gg 1/\Gamma$, where $\rho(t) \approx \text{tr}_{0,N+1} \rho(t)$ is the reduced density matrix after the tracing over the part directly affected by the dissipation [12], i.e. the reduced density matrix of interior spins.

Moreover, it can be shown that $\rho(\Gamma, t)$ commutes with the Hamiltonian (5) for suitably chosen boundary fields h_1, h_N [13], confirming that the time evolution of $\rho(\Gamma, t)$ for $t \gg 1/\Gamma$ is approximately coherent [12].

For our purposes it is enough to demonstrate that $\lim_{\Gamma \rightarrow \infty} \lim_{t \rightarrow \infty} \rho(t) = \rho_{\text{NESS}}$ satisfies

$$[\rho_{\text{NESS}}, H_{\text{bulk}} + h_1 + h_N] = 0 \quad (9)$$

$$h_1 = \vec{\sigma}_1 \cdot \hat{J} \vec{n}_l \equiv \sum_{\alpha=x,y,z} J_\alpha n_l^\alpha \sigma_1^\alpha \quad (10)$$

$$h_N = \vec{\sigma}_N \cdot \hat{J} \vec{n}_r, \quad (11)$$

(H_{bulk} given by (6)), so we shall sketch a proof here. To that end, we expand the steady state solution $\rho(\Gamma)$ of (7) in powers of $1/\Gamma$, $\rho(\Gamma) = \rho_0 + \Gamma^{-1} \rho_1 + \Gamma^{-2} \rho_2 + \dots$. Substituting into (7) we obtain a set of conditions $i[H, \rho_k] = (\mathcal{D}_{L_1} + \mathcal{D}_{L_2})[\rho_{k+1}]$, for $k = 0, 1, \dots$. These conditions are nontrivial since the operator $(\mathcal{D}_{L_1} + \mathcal{D}_{L_2})$ has nonzero kernel of the form $\rho_l \otimes X \otimes \rho_r$ where X is an arbitrary matrix. In all orders, the necessary and sufficient condition for the existence of ρ_{n+1} is $\text{tr}_{0,N+1}[H, \rho_n] = 0$. In the leading order $n = 0$, a substitution of $\rho_0 = \rho_l \otimes \rho_{\text{NESS}} \otimes \rho_r$ into $\text{tr}_{0,N+1}[H, \rho_0] = 0$ leads to (9)-(11). The Hamiltonian (9) is called a dissipation-projected Hamiltonian [12]. Thus we obtain the property (A) (2).

Remark 1. We proved that the eigenstates of Zeno NESS for boundary-driven integrable spin chains are given by integrable Hamiltonian with fine-tuned boundary fields h_1, h_N . Note that due to (10), (11) the conditions

$$\min_\alpha J_\alpha \leq \|h_1\|, \quad \|h_N\| \leq \max_\alpha J_\alpha \quad (12)$$

are always satisfied, restricting the norm of “permissible” boundary fields in (9).

To show the property (B) is more involved as it requires, to start with, a description of the relaxation mechanism of internal spins towards the steady state, $\rho(t) \rightarrow \rho_{\text{NESS}}$ for $t \gg 1/\Gamma$. This needs writing down a Dyson expansion of the time-dependent solution of the Lindblad Master equation (7) using $1/\Gamma \ll 1$ as a perturbation parameter. The procedure is explained in detail in [12, 13], while here we give an outline. The first two orders of the Dyson expansion yield an effective Lindblad Master equation for internal spins $\rho(t) = \text{tr}_{0,N+1}\rho(t)$ for $t \gg 1/\Gamma$ [13],

$$\frac{\partial \rho(\Gamma, t)}{\partial t} = -i[H_D, \rho] + \frac{1}{\Gamma} (\mathcal{D}_{g_l}[\rho] + \mathcal{D}_{g_r}[\rho]), \quad (13)$$

where $H_D \equiv H_{\text{bulk}} + h_1 + h_N$ is the dissipation-projected Hamiltonian, and g_l, g_r are effective Lindblad operators, explicitly given by:

$$g_l = \text{tr}_{0,N+1} [(\langle \psi_l \rangle \langle \psi_l^\perp | \otimes I^{\otimes N+1}) H] = \text{tr}_0 [\langle \psi_l^\perp | \vec{\sigma} | \psi_l \rangle \otimes \hat{J} \vec{\sigma}] \otimes I^{\otimes N-1}, \quad (14)$$

$$g_r = \text{tr}_{0,N+1} [(I^{\otimes N+1} \otimes |\psi_r \rangle \langle \psi_r^\perp|) H] = I^{\otimes N-1} \otimes \text{tr}_1 [\hat{J} \vec{\sigma} \otimes \langle \psi_r^\perp | \vec{\sigma} | \psi_r \rangle]. \quad (15)$$

Note that the dissipative part in (13) is of the order $1/\Gamma$, in contrast to (7) where it is of order Γ . Thus, indeed,

the effective time evolution of the bulk is approximately coherent while the relaxation is proportional to $1/\Gamma$.

Due to (9) the NESS can be written in the basis of eigenstates $|\alpha\rangle$ of $H_{\text{bulk}} + h_1 + h_N$,

$$\rho_{\text{NESS}} = \sum_\alpha \nu_\alpha |\alpha\rangle \langle \alpha|. \quad (16)$$

Assuming orthonormality $\langle \alpha | \beta \rangle = \delta_{\alpha\beta}$, and multiplying (13) by $\langle \alpha |$ from the left and by $|\alpha\rangle$ from the right, one obtains a closed system for the populations $\nu_\alpha(t) = \langle \alpha | \rho(t) | \alpha \rangle$:

$$\Gamma \frac{\partial \nu_\alpha(t)}{\partial t} = \sum_{\beta \neq \alpha} w_{\beta\alpha} \nu_\beta - \nu_\alpha \sum_{\beta \neq \alpha} w_{\alpha\beta}, \quad \alpha = 1, 2, \dots \quad (17)$$

$$w_{\beta\alpha} = |\langle \alpha | g_l | \beta \rangle|^2 + |\langle \alpha | g_r | \beta \rangle|^2. \quad (18)$$

Quantities $\nu_\alpha(t) = \langle \alpha | \rho(t) | \alpha \rangle$ are real, nonnegative and sum up to 1, (due to normalization $\text{tr} \rho(t) = 1$), which allows to interpret them as probabilities and (17) as a classical master equation for an auxiliary classical Markov process, with renormalized rates $w_{\alpha\beta}$. The stationary solution of the auxiliary Markov process (17), i.e. solution of

$$\sum_{\beta \neq \alpha} w_{\beta\alpha} \nu_\beta - \nu_\alpha \sum_{\beta \neq \alpha} w_{\alpha\beta} = 0, \quad \alpha = 1, 2, \dots, \quad (19)$$

where all $\nu_\alpha \geq 0$ due to Perron-Frobenius theorem, yields the NESS spectrum $\{\nu_\alpha\} \equiv \{e^{-\tilde{E}_\alpha}/\tilde{Z}\}$. From (19) we can find the Zeno NESS for various \hat{J} , \vec{n}_l and \vec{n}_r . Numerically, in all cases we observe the Kolmogorov relation for the rates $w_{\alpha\beta}$

$$w_{\alpha\beta} w_{\beta\gamma} w_{\gamma\alpha} = w_{\alpha\gamma} w_{\gamma\beta} w_{\beta\alpha}. \quad (20)$$

Direct consequence of the Kolmogorov relation is the detailed balance property of the solution of (19)

$$\nu_\alpha w_{\alpha\beta} = \nu_\beta w_{\beta\alpha}. \quad (21)$$

Remark 2. The Kolmogorov relation (20) is only satisfied for pure targeted boundary states, i.e. for boundary fields obeying (10), (11) with $|\vec{n}_l| = |\vec{n}_r| = 1$. It is remarkable for our purpose since it gives a direct way to find the NESS spectrum ν_α , via (21), avoiding solution of the full linear system (19) which is in general of exponential complexity (in system size N). Even though Eq. (20) is postulated, in all specific cases its validity can be checked, or proved, a posteriori. Note that due to (21), the problem of finding Zeno NESS eigenvalues ν_α reduces to a problem of finding ratios of certain correlations of eigenstates of integrable model (5), i.e. to a problem widely studied in the literature.

Below we discuss several explicit examples, for which we find the NESS spectrum $\{\nu_\alpha\} = \{\exp(-\tilde{E}_\alpha)/\tilde{Z}\}$, and establish the dissipative dressing property (4):

(i) XXX and XXZ models with boundary qubits targeted in direction of z -axis; (ii) XXZ model with boundary targeting specific polarization in the XY-plane; (iii) XYZ model with boundary targeting in specific directions. In case (i) the corresponding effective Hamiltonian is $U(1)$ -symmetric, and in the case (ii) the $U(1)$ -symmetry is broken by non-diagonal boundary fields. Finally, the case (iii) provides an evidence for the existence of dissipatively dressed quasiparticles in the most general fully anisotropic version of the Heisenberg exchange interaction, i.e., for a XYZ spin chain, where $U(1)$ symmetry is broken already at the level of the bulk Hamiltonian. The original and modified dispersion relations, for all three cases (i), (ii), (iii) constitute our main results and are listed in the next section.

III. DISSIPATIVE DRESSING OF QUASIPARTICLE DISPERSION: XXX, XXZ, XYZ MODELS WITH BOUNDARY DRIVING

XXX model with sink and source.— The dissipation-projected Hamiltonian with isotropic bulk exchange interaction and boundary fields along z -axis $h_1 = -\sigma_1^z$, $h_N = \sigma_N^z$,

$$H_D = \sum_{n=1}^{N-1} \vec{\sigma}_n \cdot \vec{\sigma}_{n+1} - \sigma_1^z + \sigma_N^z \quad (22)$$

describes the effective dynamics (13) of internal spins in an isotropic Heisenberg model of length $N+2$ where the first and the last spin are projected onto spin-down state $|\downarrow\rangle$ and spin-up state $|\uparrow\rangle$, respectively, i.e. $\vec{n}_l = (0, 0, -1)$, $\vec{n}_r = (0, 0, 1)$, in accordance with (10), (11). The $U(1)$ symmetry renders the Hamiltonian (22) block-diagonalizable within blocks of fixed magnetization. The eigenstates $|\alpha\rangle$ of H_D belonging to the block with magnetization $N-2M$ have energies (eigenvalues) $E_\alpha = N-1 + \sum_{j=1}^M \epsilon(u_{j,\alpha})$, where $u_{j,\alpha}$, $j = 1, \dots, M$, are Bethe rapidities, satisfying the Bethe Ansatz relations

$$\frac{u_j^{[-3]}}{u_j^{[+3]}} \left(\frac{u_j^{[+1]}}{u_j^{[-1]}} \right)^{2N+1} = \prod_{\substack{k=1 \\ k \neq j}}^M \prod_{\sigma=\pm 1} \frac{(u_j + \sigma u_k)^{[+2]}}{(u_j + \sigma u_k)^{[-2]}}, \quad (23)$$

in which we defined

$$u^{[q]} \equiv u + iq/2, \quad (24)$$

and $\epsilon(u)$ is the standard dispersion relation,

$$\epsilon(u) = -\frac{2}{u^2 + \frac{1}{4}}. \quad (25)$$

The NESS of the spin chain with boundary dissipation Fig. 1 has the form $|\downarrow\rangle\langle\downarrow| \otimes \rho_{\text{NESS}} \otimes |\uparrow\rangle\langle\uparrow|$ with ρ_{NESS} given by (4), $\tilde{E}_\alpha = \sum_{j=1}^M \tilde{\epsilon}(u_{j,\alpha})$, and the modified, or

dissipatively dressed, dispersion relation

$$\begin{aligned} \tilde{E}_\alpha &= \sum_{j=1}^M \tilde{\epsilon}(u_{j,\alpha}), \\ \tilde{\epsilon}(u) &= \log \left| \frac{u^2 + \frac{9}{4}}{u^2 + \frac{1}{4}} \right| = \log |1 - \epsilon(u)|, \end{aligned} \quad (26)$$

where $u_{j,\alpha}$ are given by the same BAE (23).

XXZ model with sink and source.— Our next example is the XXZ model

$$H_D = \sum_{n=1}^{N-1} \vec{\sigma}_n \cdot \hat{J} \vec{\sigma}_{n+1} + h_1 + h_N, \quad (27)$$

$$\hat{J} = \text{diag}(1, 1, \Delta), \quad h_1 = -\sigma_1^z \Delta, \quad h_N = \sigma_N^z \Delta. \quad (28)$$

The Hamiltonian in Eq. (27) gives an effective dynamics (13) for XXZ spin chain with z -anisotropy Δ and leftmost/rightmost spins projected onto states $|\downarrow\rangle/|\uparrow\rangle$, respectively, i.e. $\vec{n}_l = (0, 0, -1)$, $\vec{n}_r = (0, 0, 1)$, see (10), (11). For $\Delta = 1$, Eq. (27) reduces to (22). Like Eq. (22), the Hamiltonian (27) possesses the $U(1)$ symmetry. The spectrum of coherent model (27) is given by $E_\alpha = (N-1)\Delta + \sum_{j=1}^M \epsilon(u_{j,\alpha})$, where $\{u_{j,\alpha}\}$ satisfy Eq. (23) with the replacement

$$u^{[k]} \equiv \sinh(u + ik\gamma/2), \quad (29)$$

where $\cos \gamma = \Delta$, see pioneering paper of Sklyanin [14]. The NESS spectrum of the dissipation-driven model Fig. 1 is given by $\{\nu_\alpha \propto \exp(-\tilde{E}_\alpha)\}$, $\tilde{E}_\alpha = \sum_{j=1}^M \tilde{\epsilon}(u_{j,\alpha})$.

The original and dissipatively dressed dispersions are, respectively,

$$\epsilon(u) = \frac{-2 \sin^2 \gamma}{\sinh(u + \frac{i\gamma}{2}) \sinh(u - \frac{i\gamma}{2})}. \quad (30)$$

$$\begin{aligned} \tilde{\epsilon}(u) &= \log \left| \frac{\sinh(u + \frac{3i\gamma}{2}) \sinh(u - \frac{3i\gamma}{2})}{\sinh(u + \frac{i\gamma}{2}) \sinh(u - \frac{i\gamma}{2})} \right| \\ &= \log |1 - \epsilon(u)\Delta|. \end{aligned} \quad (31)$$

Setting $\gamma \rightarrow \delta$, $u \rightarrow \delta u$ and letting $\delta \rightarrow 0$ one recovers the result for the isotropic Heisenberg model (26).

XXZ model with chiral invariant subspace.— An XXZ Hamiltonian (27) with non-diagonal boundary fields

$$h_1 = \sigma_1^x, \quad h_N = \sigma_N^x \cos \varphi(M) + \sigma_N^y \sin \varphi(M), \quad (32)$$

$$\varphi(M) = (N+1-2M)\gamma, \quad \cos \gamma = \Delta, \quad (33)$$

gives an effective dynamics (13) for XXZ spin chain with anisotropy Δ and leftmost/rightmost spins projected onto fully polarized states in XY-plane $\vec{n}_l = (1, 0, 0)$, $\vec{n}_r = (\cos \varphi(M), \sin \varphi(M), 0)$. It was shown in Refs. [15, 16] that for integer values $M = 0, 1, \dots, N+1$ the Hamiltonian (32) has a chiral invariant subspace G_M . G_M is spanned by pieces of spin helices of the period $2\pi/\gamma$, and of the same helicity sign, and its dimension is $d_M = \binom{N+1}{M}$.

The Gibbs state restricted to the invariant subspace G_M has the form (1) with $\alpha = 1, \dots, d_M$ and $j = 1, \dots, M$. The integer M counts the number of kinks and is analogous to the number of spin down arrows in the $U(1)$ -invariant case (27): each state $|\alpha\rangle$ is parametrized via M Bethe rapidities $u_{j,\alpha}$, satisfying Bethe Ansatz equations:

$$\begin{aligned} & \left[\frac{\sinh(u_j + \frac{i\gamma}{2})}{\sinh(u_j - \frac{i\gamma}{2})} \right]^{2N+2} \left[\frac{\cosh(u_j - \frac{i\gamma}{2})}{\cosh(u_j + \frac{i\gamma}{2})} \right]^2 \\ &= \prod_{\sigma=\pm 1} \prod_{k \neq j}^M \frac{\sinh(u_j + \sigma u_k + i\gamma)}{\sinh(u_j + \sigma u_k - i\gamma)}, \quad j = 1, \dots, M. \quad (34) \end{aligned}$$

The energy levels of the coherent model (27), (32) and of the dissipatively constrained model E_α , $\nu_\alpha \propto \exp(-\tilde{E}_\alpha)$ are given by usual $E_\alpha = (N+1)\Delta + \sum_{j=1}^M \epsilon(u_{j,\alpha})$, $\tilde{E}_\alpha = \sum_{j=1}^M \tilde{\epsilon}(u_{j,\alpha})$, with original and dissipatively dressed dispersions

$$\epsilon(u) = \frac{-2 \sin^2 \gamma}{\sinh(u + \frac{i\gamma}{2}) \sinh(u - \frac{i\gamma}{2})}, \quad (35)$$

$$\begin{aligned} \tilde{\epsilon}(u) &= 2 \log \left| \frac{\cosh(u + \frac{i\gamma}{2}) \cosh(u - \frac{i\gamma}{2})}{\sinh(u + \frac{i\gamma}{2}) \sinh(u - \frac{i\gamma}{2})} \right| \\ &= 2 \log \left| \frac{\Delta \epsilon(v)}{2(1 - \Delta^2)} - 1 \right|. \quad (36) \end{aligned}$$

Note that the original dispersion $\epsilon(u)$ is the same as in the $U(1)$ invariant XXZ case even though the nature of the eigenstates $|\alpha\rangle$ is here completely different. Note also that after a standard substitution $e^{ip} = \frac{\sinh(u + \frac{i\gamma}{2})}{\sinh(u - \frac{i\gamma}{2})}$ the dispersion relation $\epsilon(u)$ acquires more familiar form $\epsilon(p) = 4(\cos p - \Delta)$.

All eigenstates within G_M are chiral, since they are a linear superposition of spin helix pieces with the same helicity (36). The “chiral quasiparticles” do not carry fixed magnetization as in the $U(1)$ case (27), but rather form domain walls, or kinks, on top of a chiral “background”, see [17] for more details. Equation (36) is proved in Section V, while its generalization for $M > 1$ is a conjecture based on numerics, see Appendix B.

XYZ model with chiral invariant subspace.— Finally we consider fully anisotropic XYZ spin chain

$$\begin{aligned} H_D &= \sum_{n=1}^{N-1} \vec{\sigma}_n \hat{J} \vec{\sigma}_{n+1} + h_1(\vec{n}_l) + h_N(\vec{n}_r), \quad (37) \\ \hat{J} &= \text{diag}(J_x, J_y, J_z), \end{aligned}$$

where h_1 and h_N are given by (10), (11). J_α can be parametrized in terms of two complex parameters η, τ and the Jacobi θ -functions as $\{J_x, J_y, J_z\} = \left\{ \frac{\theta_4(\eta)}{\theta_4(0)}, \frac{\theta_3(\eta)}{\theta_3(0)}, \frac{\theta_2(\eta)}{\theta_2(0)} \right\}$. Following Ref. [18], we use the shorthand notation $\theta_\alpha(u) \equiv \vartheta_\alpha(\pi u | e^{i\pi\tau})$, $\bar{\theta}_\alpha(u) \equiv$

$\vartheta_\alpha(\pi u | e^{2i\pi\tau})$. Real η and purely imaginary τ with $\text{Im}(\tau) > 0$ give real J_α .

As explained in Section II, (37) describes an effective dynamics (13) for XYZ spin chain with boundary spins dissipatively projected onto fully polarized states \vec{n}_l, \vec{n}_r . It is convenient to parametrize unit vectors \vec{n}_l, \vec{n}_r by two complex parameters $u_l = x_l + iy_l$, $u_r = x_r + iy_r$ as [19]

$$\begin{aligned} n_{l,r}^x &= -\frac{\theta_2(iy_{l,r})}{\theta_3(iy_{l,r})} \frac{\theta_1(x_{l,r})}{\theta_4(x_{l,r})}, \\ n_{l,r}^y &= -i \frac{\theta_1(iy_{l,r})}{\theta_3(iy_{l,r})} \frac{\theta_2(x_{l,r})}{\theta_4(x_{l,r})}, \\ n_{l,r}^z &= -\frac{\theta_4(iy_{l,r})}{\theta_3(iy_{l,r})} \frac{\theta_3(x_{l,r})}{\theta_4(x_{l,r})}. \end{aligned} \quad (38)$$

We focus on eigenstates of (37) within a chiral invariant subspace G_M with dimension $\binom{N+1}{M}$, which appears for $u_r = u_l + (N+1-2M)\eta$ and integer $M \in [0, N+1]$ [19]. This chiral subspace is an elliptic extension of the spin-helix based chiral subspace in the previous example. Each state $|\alpha\rangle$ within the invariant subspace is parametrized via M Bethe rapidities $\{u_{j,\alpha}\}$, which satisfy the following BAE [20]

$$\begin{aligned} & \left[\frac{\theta_1(u_j + \frac{\eta}{2})}{\theta_1(u_j - \frac{\eta}{2})} \right]^{2N+2} \frac{\theta_3(u_j + iy_l - \frac{\eta}{2})}{\theta_3(u_j - iy_l + \frac{\eta}{2})} \frac{\theta_4(u_j + x_l - \frac{\eta}{2})}{\theta_4(u_j - x_l + \frac{\eta}{2})} \\ & \times \frac{\theta_3(u_j - iy_r - \frac{\eta}{2})}{\theta_3(u_j + iy_r + \frac{\eta}{2})} \frac{\theta_4(u_j - x_r - \frac{\eta}{2})}{\theta_4(u_j + x_r + \frac{\eta}{2})} \\ &= \prod_{\sigma=\pm 1} \prod_{k \neq j}^M \frac{\theta_1(u_j + \sigma u_k + \eta)}{\theta_1(u_j + \sigma u_k - \eta)}, \quad j = 1, \dots, M. \quad (39) \end{aligned}$$

The energy of the model can be expressed in terms of Bethe rapidities $\{u_{j,\alpha}\}$ as

$$\begin{aligned} E_\alpha &= \sum_{j=1}^M \epsilon(u_{j,\alpha}) + (N+1)g(\eta) \\ &+ g\left(\frac{\tau}{2} + x_l\right) - g\left(\frac{\tau}{2} + x_r\right), \end{aligned} \quad (40)$$

$$g(u) = \frac{\theta_1(\eta)\theta'_1(u)}{\theta'_1(0)\theta_1(u)}, \quad \theta'_1(u) = \frac{\partial \theta_1(u)}{\partial u}, \quad (41)$$

where $\epsilon(u)$ is the original dispersion relation

$$\epsilon(u) = 2 \left[g(u - \frac{\eta}{2}) - g(u + \frac{\eta}{2}) \right]. \quad (42)$$

On the basis of numerical studies (see Appendix C), we conjecture that dissipative dressing effect takes place also here, i.e. the $\rho_{\text{NESS}} = \tilde{Z}^{-1} \sum_\alpha \exp(-\tilde{E}_\alpha) |\alpha\rangle \langle \alpha|$ with $\tilde{E}_\alpha = \sum_{j=1}^M \tilde{\epsilon}(u_{j,\alpha})$, where

$$\tilde{\epsilon}(u) = 2 \log \left| \frac{Q\left(\frac{1-\tau}{2} + i \text{Im} u_l, u\right)}{Q(0, u)} \right|, \quad (43)$$

$$Q(x, u) = \theta_1(x - u + \frac{\eta}{2}) \theta_1(x + u + \frac{\eta}{2}),$$

By letting $i \text{Im} u_l = \tau/2$ and $\tau \rightarrow +i\infty$, one recovers from (43) the XXZ limit (36) with $\gamma = \pi\eta$. More details are given in Appendix C.

IV. XXX/XXZ MODEL WITH SINK AND SOURCE: DERIVATION OF DISSIPATIVE DRESSING RELATIONS

The derivation of the expressions for dissipatively dressed dispersion appears rather technical as any problem having to do with finding correlation functions of interacting many-body systems. Here we show how to derive the simplest of our results, Eq. (26) for the dissipatively dressed dispersion of isotropic Heisenberg model with sink a source, in a pedagogical way.

The eigenstates of

$$H_D = \sum_{n=1}^{N-1} \vec{\sigma}_n \cdot \vec{\sigma}_{n+1} - \sigma_1^z + \sigma_N^z, \quad (44)$$

can be separated into blocks with fixed total magnetization due to $U(1)$ symmetry. Since ρ_{NESS} commutes with (44), H and ρ_{NESS} can be diagonalized simultaneously. The simplest eigenstate of H is a state with maximal possible magnetization $|0\rangle \equiv |\uparrow\uparrow\ldots\uparrow\rangle$. In the block with $M = 1, 2, \dots$ spins down the eigenstates have the form

$$|\alpha\rangle = \sum_{n=1}^N \gamma_n(u_\alpha) \sigma_n^- |0\rangle, \quad (45)$$

$$|\beta\rangle = \sum_{n_1, n_2=1}^N \gamma_{n_1, n_2}(u_{1, \beta}, u_{2, \beta}) \sigma_{n_1}^- \sigma_{n_2}^- |0\rangle, \quad (46)$$

...

Assuming non-degeneracy of the spectrum of H , ρ_{NESS} has the same eigenstates and can be written as

$$\rho_{\text{NESS}} = \nu_0 |0\rangle \langle 0| + \sum_{\alpha=1}^N \nu_\alpha^{(1)} |\alpha\rangle \langle \alpha| + \dots \quad (47)$$

where \dots denote contributions from blocks with $M > 1$. From Eqs. (14), (15), we find $g_l = \sigma_1^-$, $g_r = \sigma_N^+$.

According to detailed balance relations (21) (that can be proved a posteriori), $\nu_\alpha^{(1)}/\nu_0 = w_{0\alpha}/w_{\alpha 0}$. From (18) we find

$$\frac{w_{0\alpha}}{w_{\alpha 0}} = \frac{|\langle \alpha | \sigma_1^- |0\rangle|^2 + |\langle \alpha | \sigma_N^+ |0\rangle|^2}{|\langle 0 | \sigma_1^- | \alpha \rangle|^2 + |\langle 0 | \sigma_N^+ | \alpha \rangle|^2} \quad (48)$$

$$= \frac{|\langle \alpha | \sigma_1^- |0\rangle|^2}{|\langle 0 | \sigma_N^+ | \alpha \rangle|^2} = \left| \frac{\gamma_1}{\gamma_N} \right|^2 \quad (49)$$

In order to find the ratio γ_1/γ_N : we use the algebraic Bethe Ansatz method. Within the method, the eigenvectors of H are produced by repetitive action of a “creation” operator $\mathbb{B}(u)$ on the vacuum state $|0\rangle$. Each application of $\mathbb{B}(u)$ lowers the total magnetization by 1, so e.g. eigenstates from (45), (46) are produced as $|\alpha\rangle = \mathbb{B}(u_{1, \alpha})|0\rangle$, $|\beta\rangle = \mathbb{B}(u_{1, \beta})\mathbb{B}(u_{2, \beta})|0\rangle$. Here $u_{j, \alpha}, u_{j, \beta}$ are Bethe roots (solutions of (23)) for $M = 1$ and $M = 2$ respectively.

Let us first introduce the double-row monodromy matrix

$$T_0(u) = T_0(u) \mathcal{K}_0(u) \bar{T}_0(u), \quad (50)$$

where subscript 0 denotes the two-dimensional auxiliary space. The one-row monodromy matrices $\tau(u)$, $\bar{\tau}(u)$ and the K -matrix in Eq. (50) are defined as

$$T(u) = R_{0, N}(u) \dots R_{0, 1}(u) = \begin{pmatrix} A(u) & B(u) \\ C(u) & D(u) \end{pmatrix}, \quad (51)$$

$$\bar{T}(u) = R_{0, 1}(u) \dots R_{0, N}(u) = \begin{pmatrix} \bar{A}(u) & \bar{B}(u) \\ \bar{C}(u) & \bar{D}(u) \end{pmatrix}, \quad (52)$$

$$R_{0, n}(u) = \begin{pmatrix} uI + \frac{i}{2} \sigma_n^z & i\sigma_n^- \\ i\sigma_n^+ & uI - \frac{i}{2} \sigma_n^z \end{pmatrix}, \quad (53)$$

and

$$\mathcal{K}(u) = \text{diag} \left\{ u^{[-3]}, -u^{[1]} \right\}. \quad (54)$$

The “eigenstates” creation operator $\mathbb{B}(u)$ is an element of $\mathcal{T}(u)$:

$$\mathbb{B}(u) = [\mathcal{T}(u)]_2^1 = u^{[-3]} A(u) \bar{B}(u) - u^{[1]} B(u) \bar{D}(u). \quad (55)$$

The following relation

$$T_1(u) R_{1, 2}(2u - \frac{i}{2}) \bar{T}_2(u) = \bar{T}_2(u) R_{1, 2}(2u - \frac{i}{2}) T_1(u), \quad (56)$$

leads to

$$A(u) \bar{B}(u) = \frac{2u - i}{2u} \bar{B}(u) A(u) - \frac{i}{2u} B(u) \bar{D}(u). \quad (57)$$

Then, we derive

$$\mathbb{B}(u_{1, \alpha}) = \frac{u^{[-3]} u^{[-1]}}{u} \bar{B}(u) A(u) - \frac{u^{[3]} u^{[-1]}}{u} B(u) \bar{D}(u). \quad (58)$$

From the explicit form of the one-row monodromy matrices, we obtain

$$A(u) |0\rangle = \left(u^{[1]} \right)^N |0\rangle, \quad (59)$$

$$\bar{D}(u) |0\rangle = \left(u^{[-1]} \right)^N |0\rangle, \quad (60)$$

$$\bar{B}(u) |0\rangle = i \sum_{m=1}^N F_m(u) \sigma_m^- |0\rangle, \quad (61)$$

$$B(u) |0\rangle = i \sum_{m=1}^N F_{N-m+1}(u) \sigma_m^- |0\rangle, \quad (62)$$

$$F_m(u) = \left(u^{[1]} \right)^{m-1} \left(u^{[-1]} \right)^{N-m}. \quad (63)$$

The Bethe state $\mathbb{B}(u)|0\rangle$ can be expanded as

$$\begin{aligned}\mathbb{B}(u)|0\rangle &= i \frac{u^{[-3]}u^{[-1]}}{u} \left(u^{[1]}\right)^N \sum_{m=1}^N F_m(u) \sigma_m^- |0\rangle \\ &- i \frac{u^{[3]}u^{[-1]}}{u} \left(u^{[-1]}\right)^N \sum_{m=1}^N F_{N-m+1}(u) \sigma_m^- |0\rangle.\end{aligned}\quad (64)$$

With the help of Eq. (64), it can be derived that

$$\gamma_1(u) = 2 \left(u^{[-1]}\right)^N \left(u^{[1]}\right)^{N-1}, \quad (65)$$

$$\begin{aligned}\gamma_N(u) &= \frac{iu^{[-3]}u^{[-1]}\left(u^{[1]}\right)^{2N-1} - iu^{[3]}\left(u^{[-1]}\right)^{2N}}{u} \\ &\stackrel{(23)}{=} 2 \left(u^{[-1]}\right)^{2N} u^{[3]} \left(u^{[1]}\right)^{-2}.\end{aligned}\quad (66)$$

One can thus obtain the ratio

$$\frac{\gamma_1^2(u)}{\gamma_N^2(u)} = \left(\frac{u^{[1]}}{u^{[-1]}}\right)^{2N} \left(\frac{u^{[1]}}{u^{[3]}}\right)^2 \stackrel{(23)}{=} \frac{u^{[1]}u^{[-1]}}{u^{[3]}u^{[-3]}}, \quad (67)$$

leading to (26) for $M = 1$.

Proceeding iteratively for $M = 2, 3, \dots$ one can verify the general validity of (26).

The effects of a dissipative dressing on the NESS spectrum can be seen already in the one-particle sector $M = 1$. Notably, the bare (original) quasiparticle dispersion $\epsilon(u)$ has a singularity at $u = \pm i/2$, while dissipatively dressed quasiparticle dispersion $\tilde{\epsilon}(u)$ (67) retains the singularity at $u = \pm i/2$ and acquires an extra singularity at $u = \pm 3i/2$. In the following we show that some solutions of BAE lie exponentially close to the extra singularity $u = \pm 3i/2$, drastically modifying the NESS spectrum \tilde{E}_α with respect to the H spectrum E_α .

The sector $M = 1$, contains N Bethe eigenstates $|\alpha\rangle$ parametrized by the solutions u_α , $\alpha = 1, \dots, N$, of the BAE (23). Among the N BAE solutions there are always $N-1$ real solutions, say u_2, \dots, u_N , and one boundary localized imaginary solution u_1 , lying exponentially close to the extra singularity due to dissipative dressing, namely, $u_1 = i(3/2 + O(2^{-N}))$, see the top panel of Fig. 2. Explicitly, from (23) we find $u_1 - 3i/2 \equiv \delta = 3i2^{-2N-1}(1 + O(N\delta))$. The corresponding dressed energy $\tilde{\epsilon}(u_1)$ is drastically renormalized by the singularity, acquiring a negative amplitude linearly growing with system size, $\tilde{\epsilon}(u_1) \approx -2(N+1) \log 2 + \log 9$, see (80). On the other hand, for plane wave type (real u_j) BAE solutions, the dressed and original energies are comparable. As a result, $e^{-\tilde{\epsilon}(u_1)} \gg e^{-\tilde{\epsilon}(u_\alpha)}$ for $\alpha > 1$, and in the NESS, the boundary localized Bethe eigenstate $|\alpha = 1\rangle$ comes with an exponentially large (in system size N) relative weight in the sum (3) with respect to the plane wave $M = 1$ eigenstates $|\alpha\rangle$, see Fig. 2. In sectors with several quasiparticles $M > 1$ we observe similar phenomenon which leads to an overall subextensive scaling of the von-Neumann entropy of the NESS (3) with the system size, see [6].

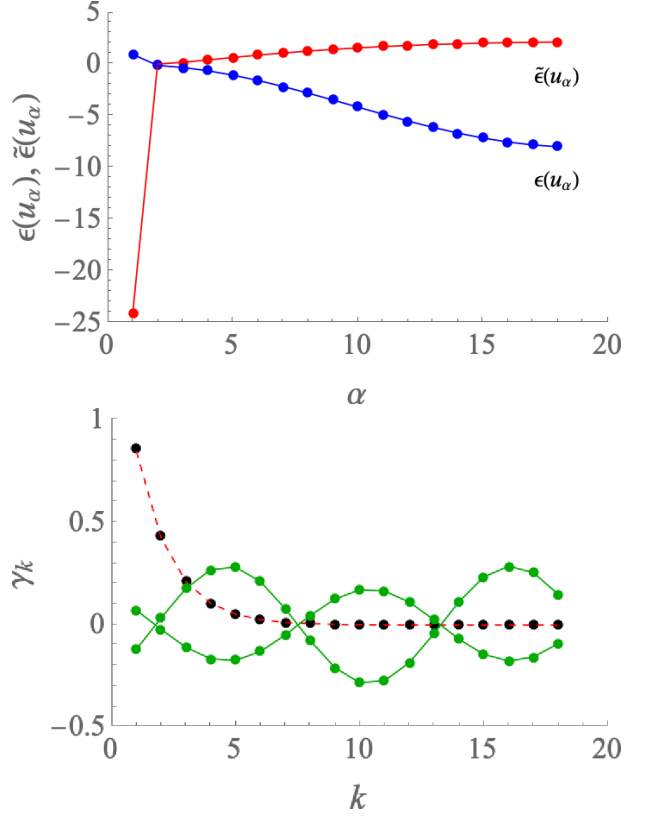


Fig. 2. Top panel: quasiparticle energies $\epsilon(u_\alpha)$ (blue joined points) and their dissipative dressing $\tilde{\epsilon}(u_\alpha)$ (red joined points) in the XXX model with $N = 18$ spin, in the block with one magnon $M = 1$. The state $\alpha = 1$ is a localized Bethe state with $u_1 \simeq 3i/2 + ie^{-24.5}$. Bottom panel: coefficients γ_k of the normalized localized Bethe state $|\alpha = 1\rangle = \sum_{k=1}^N \gamma_k \sigma_k^- |0\rangle$ (black empty circles). The dashed red line is the fit $\gamma_k = 1.7 \times 2^{-k}$. The green joined points are the coefficients $\text{Re } \gamma_k$ and $\text{Im } \gamma_k$ for the plain-wave like Bethe state with $u_4 \approx 1.78139$.

Trigonometric case. — We pass to the trigonometric XXZ case (27) by redefining the functions $u^{[k]}$ as (29). The dispersion relation of the quasiparticles has form

$$\epsilon(u) = -\frac{2 \sin^2 \gamma}{u^{[1]}u^{[-1]}} \quad (68)$$

and the XXZ eigenvalues are

$$E = \sum_{j=1}^M \epsilon(u_j) + (N-1) \cos \gamma, \quad (69)$$

where $\{u_j\}$ are solutions of BAE (23), with redefinition (29). The one-particle wave function is given by the expression (64) with the replacements (29) and $i \rightarrow i \sin \gamma$.

Repeating the calculations, we find

$$\frac{\nu_\alpha^{(1)}}{\nu_0} = \frac{u^{[1]}u^{[-1]}}{u^{[3]}u^{[-3]}} \quad (70)$$

leading to (31) for $M = 1$.

Proceeding analogously for $M = 2, 3, \dots$ one can verify the validity of (31), and consequently, of (26), iteratively. In [6] we obtain the result (31) in an alternative way, expressing the operators g_l, g_r in terms of $\mathbb{B}(u)$ and using the commutation relation between the monodromy matrix elements.

Let us analyze the BAE solutions for $M = 1$ case in more detail. The corresponding Bethe states can be rewritten in terms of the quasi-momentum p as

$$\sum_{n=1}^N \mathcal{A}_n(p) \sigma_n^- |0\rangle, \quad (71)$$

$$\mathcal{A}_n(p) = (e^{ip} - 2\Delta) e^{inp} - (1 - 2\Delta e^{ip}) e^{i(1-n)p}, \quad (72)$$

where p satisfies

$$e^{i(2N+1)p} (e^{ip} - 2\Delta) - (1 - 2\Delta e^{ip}) = 0. \quad (73)$$

Most solutions for p of (73) are real. However, in some cases, Eq. (73) has an imaginary solution. Indeed, let us define a function

$$\mathcal{W}(x) = x^{(2N+1)}(x - 2\Delta) - (1 - 2\Delta x). \quad (74)$$

One can easily check that

$$\begin{aligned} \mathcal{W}(1) &= 0, & \mathcal{W}(\frac{1}{2\Delta}) &= (1 - 4\Delta^2)(2\Delta)^{-2N-2}, \\ \mathcal{W}(2\Delta) &= 4\Delta^2 - 1, & \mathcal{W}'(1) &= 2 + 2N(1 - 2\Delta). \end{aligned} \quad (75)$$

Once

$$\Delta > \frac{1}{2}, \quad N > \frac{1}{2\Delta - 1} \quad (76)$$

we have

$$\mathcal{W}(\frac{1}{2\Delta}) < 0, \quad \mathcal{W}(1) = 0, \quad \mathcal{W}'(1) < 0. \quad (77)$$

Therefore, $\mathcal{W}(x) = 0$ has a solution in the interval $(\frac{1}{2\Delta}, 1)$ under the condition (76). And, from (74), the root approaches $\frac{1}{2\Delta}$ as N increases. Since $\mathcal{W}(e^{ip}) = 0$ is exactly the BAE (73), this implies an imaginary root p with $e^{ip} \approx \frac{1}{2\Delta}$ (or equivalently, $u \approx -\frac{3i\gamma}{2}$). When N is large enough, this imaginary p will give a localized state with

$$\mathcal{A}_n(p) \approx \left(\frac{1}{2\Delta} - 2\Delta \right) \left(\frac{1}{2\Delta} \right)^n. \quad (78)$$

The dressed energy in terms of p is

$$\begin{aligned} &\log |e^{-ip} (e^{ip} - 2\Delta) (1 - 2\Delta e^{ip})| \\ &\stackrel{(73)}{=} \log |e^{2iNp} (e^{ip} - 2\Delta)^2|. \end{aligned} \quad (79)$$

For the imaginary solution $e^{ip} \approx \frac{1}{2\Delta}$ for large N , the dressed energy $\tilde{\epsilon}(p)$ becomes

$$\begin{aligned} \tilde{\epsilon} &\approx \log |(2\Delta)^{-2N-2} (1 - 4\Delta^2)^2| \\ &= -2(N+1) \log(2\Delta) + 2 \log(4\Delta^2 - 1). \end{aligned}$$

In particular, for $\Delta = 1$ we obtain

$$\tilde{\epsilon} \approx -2(N+1) \log 2 + \log 9. \quad (80)$$

V. XXZ MODEL WITH CHIRAL INVARIANT SUBSPACE: DERIVATION OF DISSIPATIVELY DRESSED DISPERSION (36)

Like in the previous section, we first prove (36) for the single quasiparticle $M = 1$ sector.

Let us introduce the following family of chiral states:

$$\begin{aligned} \langle \Phi(n_1, \dots, n_M) | &= \exp \left[i\gamma \sum_k n_k \right] \bigotimes_{l_1=1}^{n_1} \phi(l_1) \\ &\bigotimes_{l_2=n_1+1}^{n_2} \phi(l_2 - 2) \cdots \bigotimes_{l_{M+1}=n_M+1}^N \phi(l_{M+1} - 2M), \\ \phi(n) &= \frac{1}{\sqrt{2}} (1, e^{-in\gamma}). \end{aligned} \quad (81)$$

Then, the set

$$\langle \Phi(n_1, \dots, n_M) |, \quad 0 \leq n_1 < n_2 < \dots < n_M \leq N,$$

forms an invariant subspace of the Hamiltonian (27),(32) [15]. A chiral analog of coordinate Bethe Ansatz [17] then leads to the consistency conditions which have the form of standard BAE (34). We aim at finding NESS eigenvalues, corresponding to the invariant subspace eigenstates $|\alpha\rangle$ of (27),(32). According to (21), the ratio of the NESS eigenvalues for the associated dissipative problem (Fig. 1) is given by

$$\frac{\nu_\alpha}{\nu_\beta} = \frac{w_{\beta\alpha}}{w_{\alpha\beta}} = \frac{|\langle \alpha | g_l | \beta \rangle|^2 + |\langle \alpha | g_r | 0 \rangle|^2}{|\langle \beta | g_l | \alpha \rangle|^2 + |\langle \beta | g_r | \alpha \rangle|^2}, \quad (82)$$

with operators $g_{l,r}$ computed from (14),(15):

$$\begin{aligned} g_l &= G_L \otimes I^{\otimes N-1}, \quad g_r = I^{\otimes N-1} \otimes G_R, \\ G_{L,R} &= \begin{pmatrix} \cos \gamma & -e^{-i\varphi_{l,r}} \\ e^{i\varphi_{l,r}} & -\cos \gamma \end{pmatrix}, \\ \varphi_l &= 0, \quad \varphi_r = \varphi(M). \end{aligned} \quad (83)$$

Let us calculate (82) for $M = 1$, where the Bethe states have the form [15]

$$\langle \alpha | = \sum_{n=0}^N \langle \Phi(n) | f_n(p^{(\alpha)}), \quad (84)$$

$$f_n(p) = e^{i\chi+inp} + e^{-i\chi-inp}, \quad e^{2i\chi(p)} = \frac{\Delta - e^{ip}}{e^{-ip} - \Delta}. \quad (85)$$

Here, the “quasimomentum” p and the rapidity u from (34) are related by standard relation

$$e^{ip} = \frac{\sinh(u + \frac{i\gamma}{2})}{\sinh(u - \frac{i\gamma}{2})}. \quad (86)$$

In terms of p , BAE (34) for $M = 1$ acquire a simple form

$$e^{2iNp} e^{4i\chi} = 1. \quad (87)$$

All solutions p_α of Eq. (87) are real, meaning that also $f_n(p_\alpha)$ are all real.

To compute the expressions $\langle \alpha | g_l | \beta \rangle$ in (82) we note the following property:

$$\begin{aligned} g_l |\Phi(n)\rangle &= \kappa(2\delta_{n,0} - 1) |\Phi(n)\rangle, \\ g_r |\Phi(n)\rangle &= \kappa(1 - 2\delta_{n,N}) |\Phi(n)\rangle, \\ \kappa &= i \sin \gamma. \end{aligned} \quad (88)$$

While the eigenstates $|\alpha\rangle$ in (84) are orthonormal, the chiral states $|\Phi(n)\rangle$ are not,

$$\langle \Phi(n) | \Phi(m) \rangle = \Delta^{|n-m|}. \quad (89)$$

For further calculations we set

$$p \equiv p_\alpha, \quad p' \equiv p_\beta, \quad \chi \equiv \chi(p_\alpha), \quad \chi' \equiv \chi(p_\beta) \quad (90)$$

for notational simplicity. Using (88), (89), $\langle \alpha | \beta \rangle = 0$ and $f_n^* = f_n$ we obtain

$$\langle \alpha | g_l | \beta \rangle = 2\kappa f_0(p') \sum_{n=0}^N f_n(p) \Delta^n, \quad (91)$$

$$\langle \alpha | g_r | \beta \rangle = -2\kappa f_N(p') \sum_{n=0}^N f_{N-n}(p) \Delta^n. \quad (92)$$

From (87), we readily find

$$f_{N-n}(p) = \pm f_n(p). \quad (93)$$

It follows that

$$| \langle \alpha | g_l | \beta \rangle | = | \langle \alpha | g_r | \beta \rangle |, \quad (94)$$

and consequently

$$\frac{\nu_\alpha}{\nu_\beta} = \frac{|\langle \alpha | g_l | \beta \rangle|^2}{|\langle \beta | g_l | \alpha \rangle|^2}. \quad (95)$$

Performing summation in (91) we obtain

$$\begin{aligned} \langle \alpha | g_l | \beta \rangle &= 2\kappa f_0(p') \sum_{n=0}^N f_n(p) \Delta^n \\ &= 2\kappa f_0(p') \left(e^{i\chi} \frac{1 - z_+^{N+1}}{1 - z_+} + e^{-i\chi} \frac{1 - z_-^{N+1}}{1 - z_-} \right), \\ z_\pm &= e^{\pm ip} \Delta. \end{aligned}$$

Remarkably, due to BAE (87), the N -dependence in the above vanishes:

$$\begin{aligned} &e^{i\chi} \frac{z_+^{N+1}}{1 - z_+} + e^{-i\chi} \frac{z_-^{N+1}}{1 - z_-} \\ &= z_-^{N+1} e^{-i\chi} \left(\frac{e^{2iNp+2i\chi} e^{2ip}}{1 - z_+} + \frac{1}{1 - z_-} \right) \\ &= z_-^{N+1} e^{-i\chi} \left(\frac{e^{-2i\chi} e^{2ip}}{1 - z_+} + \frac{1}{1 - z_-} \right) \\ &= z_-^{N+1} e^{-i\chi} \left(e^{-ip} \frac{1 - z_+}{\Delta - e^{ip}} \frac{e^{2ip}}{1 - z_+} + \frac{1}{1 - z_-} \right) \\ &= 0. \end{aligned} \quad (96)$$

So we obtain

$$\frac{\langle \alpha | g_l | \beta \rangle}{2\kappa} = f_0(p') \left(\frac{e^{i\chi}}{1 - z_+} + \frac{e^{-i\chi}}{1 - z_-} \right). \quad (97)$$

From (85) we have

$$e^{i\chi} (e^{-ip} - \Delta) = e^{-i\chi} (\Delta - e^{ip}),$$

and for the real part

$$\cos(\chi - p) = \Delta \cos \chi. \quad (98)$$

Noting $f_0(p') = 2 \cos \chi'$ and using (98), after some straightforward algebra we obtain

$$\langle \alpha | g_l | \beta \rangle = \frac{8\kappa(\Delta^{-1} - \Delta) \cos \chi' \cos \chi}{\Delta + \Delta^{-1} - 2 \cos p}. \quad (99)$$

The expression for $\langle \beta | g_l | \alpha \rangle$ is obtained from the above by substitutions $p \leftrightarrow p'$, $\chi \leftrightarrow \chi'$, yielding

$$\frac{\langle \alpha | g_l | \beta \rangle}{\langle \beta | g_l | \alpha \rangle} = \frac{\Delta + \Delta^{-1} - 2 \cos p'}{\Delta + \Delta^{-1} - 2 \cos p}. \quad (100)$$

Notably, the Kolmogorov relation (20) follows from Eq. (100), justifying aposteriori the assumption (82).

Restoring the original notations (90) we get

$$\frac{\nu_\alpha}{\nu_\beta} = \frac{|\Delta + \Delta^{-1} - 2 \cos p_\beta|^2}{|\Delta + \Delta^{-1} - 2 \cos p_\alpha|^2}. \quad (101)$$

Finally, using $\log \frac{\nu_\beta}{\nu_\alpha} = \tilde{E}_\alpha - \tilde{E}_\beta = \tilde{\epsilon}(u_\alpha) - \tilde{\epsilon}(u_\beta)$, and (86), the Eq. (101) reduces to (36).

Fig. 3 shows dissipatively dressed and original energies for the multiplet from chiral invariant subspace with $M = 1$. We see that the the dissipative dressing reverses the order of the contributions in the respective NESS with respect to the Gibbs state, (for $\epsilon(u_\alpha) < \epsilon(u_\beta)$, $\tilde{\epsilon}(u_\alpha) > \tilde{\epsilon}(u_\beta)$). However, unlike in the XXZ model with diagonal boundary fields, we do not see drastic renormalization effects for some eigenstates like in Fig. 2. This happens because all Bethe roots u_j are now real, and therefore cannot approach singularities of $\tilde{\epsilon}(u)$, lying on the imaginary axis, as it happened in the “sink and source” case (Fig. 2).

Even though there are no principal difficulties to extend the above calculations for larger M using the chiral Bethe Ansatz method [17], the analytic expressions become difficult to handle because of the non-orthogonality of the chiral basis vectors (81). For $M > 1$ the validity of (36) is thus checked numerically, see Appendix B.

VI. DISCUSSION

In summary, we have found and described a surprising effect of dissipative dressing of quasiparticle dispersion relation, in integrable spin chains attached to strongly dissipative baths. So far we have been able to find a rigorous

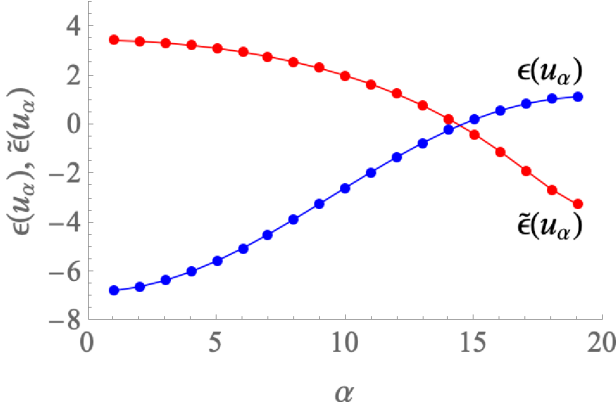


Fig. 3. Quasiparticle energies $\epsilon(u_\alpha)$ (blue joined points) and dissipatively dressed ones $\tilde{\epsilon}(u_\alpha)$ (red joined points) in the XXZ model with chiral invariant subspace, in the block with one kink $M = 1$. Parameters: $N = 18$, $\Delta = 0.7$. There are no localized states: all the amplitudes are plain-wave like, data not shown.

proof only for the $U(1)$ -symmetric “sink and source” case (31), which is valid for all eigenstates, see the companion paper [6]. However, the effect of dissipative dressing is definitely present in other integrable systems as discussed in the present paper, including fully anisotropic XYZ model, as suggested by firm numerical evidence. For all the cases, we find the dissipatively dressed dispersion relation (energy of quasiparticle) of the form

$$\tilde{\epsilon}(u) \sim \log(\epsilon(u)/f(u)), \quad (102)$$

where u is a Bethe rapidity, $\epsilon(u)$ is the original quasiparticle dispersion, and $f(u)$ contains an additional sin-

gularity. While for the XXZ model the property (102) is obvious by comparison of (31) and (36) with (35), for the XYZ model (102) seems not obviously true. However, also for the XYZ case, our numerical data confirm the validity of (102) where $f(u)$ depends on extra complex parameter (to be reported elsewhere).

Using the dissipatively dressed dispersion relation as a key input we have been able to diagonalize the steady state density operators of boundary dissipatively driven integrable quantum spin chains in the limit of large dissipation, alias the Zeno regime, by employing the Bethe Ansatz of a related dissipation-projected Hamiltonian. We have thus discovered a simple but surprising phenomenon of “dissipative dressing” of quasiparticle energies in integrable coherent systems exposed to boundary dissipation.

Our results should have applications in state engineering and dissipative state preparation. Moreover, we expect analogous emergent integrability of the steady state density operators in the discrete-time case of an integrable Floquet XXX/XXZ/XYZ circuits, where boundary dissipation can be conveniently implemented by the so-called reset channel [11, 21].

ACKNOWLEDGMENTS

V.P. and T.P. acknowledge support by ERC Advanced grant No. 101096208 – QUEST, and Research Program P1-0402 and Grant N1-0368 of Slovenian Research and Innovation Agency (ARIS). V.P. is also supported by Deutsche Forschungsgemeinschaft through DFG project KL645/20-2. X.Z. acknowledges financial support from the National Natural Science Foundation of China (No. 12204519).

[1] H. Bethe, *Zeitschrift für Physik* **71**, 205 (1931).

[2] R. J. Baxter, *Exactly solved models in statistical mechanics* (Courier Corporation, 2007).

[3] L. A. Takhtadzhan and L. D. Faddeev, *Rush. Math. Surveys* **34**, 11 (1979).

[4] E. K. Sklyanin, L. A. Takhtadzhyan, and L. D. Faddeev, *Theor. Math. Phys.* **40**, 688 (1980).

[5] E. K. Sklyanin, *Progress of Theoretical Physics Supplement* **118**, 35 (1995).

[6] V. Popkov, X. Zhang, C. Presilla, and T. Prosen, [arXiv:2408.09302](https://arxiv.org/abs/2408.09302).

[7] J. Cao, S. Cui, W.-L. Yang, K. Shi, and Y. Wang, *Nucl. Phys. B* **886**, 185 (2014).

[8] Y. Wang, W.-L. Yang, J. Cao, and K. Shi, *Off-Diagonal Bethe Ansatz for Exactly Solvable Models* (Springer, 2016).

[9] V. Popkov, D. Karevski, and G. M. Schütz, *Phys. Rev. E* **88**, 062118 (2013).

[10] G. T. Landi, E. Novais, M. J. de Oliveira, and D. Karevski, *Phys. Rev. E* **90**, 042142 (2014).

[11] X. Mi, A. A. Michailidis, S. Shabani, K. C. Miao, Klimov, et al., *Science* **383**, 1332 (2024).

[12] P. Zanardi and L. Campos Venuti, *Phys. Rev. Lett.* **113**, 240406 (2014).

[13] V. Popkov, S. Essink, C. Presilla, and G. Schütz, *Phys. Rev. A* **98**, 052110 (2018).

[14] E. K. Sklyanin, *J. Phys. A* **21**, 2375 (1988).

[15] X. Zhang, A. Klümper, and V. Popkov, *Phys. Rev. B* **103**, 115435 (2021).

[16] V. Popkov and M. Salerno, *Europhysics Lett.* **140**, 11004 (2022).

[17] X. Zhang, A. Klümper, and V. Popkov, *Phys. Rev. B* **104**, 195409 (2021).

[18] E. T. Whittaker and G. N. Watson, *A course of modern analysis* (Cambridge University Press, 1950).

[19] X. Zhang, A. Klümper, and V. Popkov, *Phys. Rev. B* **106**, 075406 (2022).

[20] W.-L. Yang and Y.-Z. Zhang, *Nucl. Phys. B* **744**, 312 (2006).

[21] V. Popkov and T. Prosen, [arXiv:2502.06731](https://arxiv.org/abs/2502.06731).

[22] J. Cao, H.-Q. Lin, K.-J. Shi, and Y. Wang, *Nucl. Phys. B* **663**, 487 (2003).

[23] R. I. Nepomechie, *J. Phys. A* **37**, 433 (2003).

APPENDICES

This Appendix part contains three sections. In Appendix A we sketch a derivation of the Lindblad Master equation starting from brickwall qubit circuit. Appendices B and C contain some details and Tables for XXZ and XYZ model with chiral invariant subspaces.

Appendix A: Lindblad Master equation evolution as a limit of a brickwall unitary circuit

Here we describe a brickwall unitary circuit leading to the Lindblad Master equation Eq.(7) with an XXX Hamiltonian in the continuous time (Trotter) limit.

It is described by a two step discrete time protocol, schematically shown in Fig. A-1. Assuming N being odd, the discrete evolution has the following form

$$\mathcal{M} = \mathcal{M}_{\text{odd}} \mathcal{M}_{\text{even}} \quad (\text{A-1})$$

$$\mathcal{M}_{\text{even}}[\rho] = \sum_{j=1}^2 F_j(\epsilon) U_{01} U_{23} \dots U_{N-1, N} \rho U_{01}^\dagger U_{23}^\dagger \dots U_{N-1, N}^\dagger F_j(\epsilon)^\dagger \quad (\text{A-2})$$

$$\mathcal{M}_{\text{odd}}[\rho] = \sum_{j=1}^2 K_j(\epsilon) U_{12} U_{34} \dots U_{N, N+1} \rho U_{12}^\dagger U_{34}^\dagger \dots U_{N, N+1}^\dagger K_j(\epsilon)^\dagger \quad (\text{A-3})$$

$$U_{n, n+1} = \frac{1 - i\tau P_{n, n+1}}{1 + i\tau}, \quad P_{n, n+1} = \frac{1}{2} (I + \vec{\sigma}_n \cdot \vec{\sigma}_{n+1}) \quad (\text{A-4})$$

where $P_{n, n+1}$ is a permutation, and the Krauss gates $K_j(\epsilon)$, τ is a real number, $F_j(\epsilon)$, $0 \leq \epsilon < 1$ act on spins 0 and $N+1$ respectively, see Fig. A-1. Explicitly the Krauss gates are given by

$$F_1(\epsilon) = \sqrt{1-\epsilon} \sigma_{N+1}^+, \quad F_2(\epsilon) = \begin{pmatrix} 1 & 0 \\ 0 & \sqrt{\epsilon} \end{pmatrix} \quad (\text{A-5})$$

$$K_1(\epsilon) = \sqrt{1-\epsilon} \sigma_0^-, \quad K_2(\epsilon) = \begin{pmatrix} \sqrt{\epsilon} & 0 \\ 0 & 1 \end{pmatrix} \quad (\text{A-6})$$

The Krauss gate $K(\epsilon)[\cdot] = \sum_{j=1}^2 K_j[\cdot] K_j^\dagger$ is a linear operation on a 2×2 matrices. Its eigenstates ψ_k and eigenvalues λ_k are $\psi_0 = |\uparrow\rangle\langle\uparrow|$, $\psi_1 = \sigma^z$, $\psi_2 = \sigma^+$, $\psi_3 = \sigma^-$, and $\lambda_0 = 1, \lambda_1 = \epsilon, \lambda_2 = \lambda_3 = \lambda_4 = \sqrt{\epsilon}$. On the other hand, the exponentiated Lindblad operator $e^{\Gamma t \mathcal{D}_{\sigma^-}}[\cdot]$ with \mathcal{D}_L given by (8) has exactly the same eigenvectors $\{\psi_k\}$ and the eigenvalues $\mu_0 = 1, \mu_1 = e^{-\Gamma t}, \mu_2 = \mu_3 = e^{-\Gamma t/2}$. We thus obtain, that an application of a Krauss gate n times

$$K^n(\epsilon)[\cdot] = e^{\Gamma t \mathcal{D}_{\sigma^-}}[\cdot], \quad \text{if } \epsilon = e^{-\Gamma t/n}. \quad (\text{A-7})$$

Analogously,

$$F^n(\epsilon)[\cdot] = e^{\Gamma t \mathcal{D}_{\sigma^+}}[\cdot], \quad \text{if } \epsilon = e^{-\Gamma t/n}. \quad (\text{A-8})$$

The boundary driven Lindblad equation (7) is obtained in the limit

$$\tau = t/n \ll 1, \quad (\text{A-9})$$

$$U \approx I - i\tau P \quad (\text{A-10})$$

$$\mathcal{M}[\rho(t)] \equiv \rho(t + \tau) \quad (\text{A-11})$$

so that $\lim_{\tau \rightarrow 0} (\mathcal{M}[\rho(t)] - \rho(t))/\tau = \frac{d\rho}{dt}$ after a straightforward algebra leads to the differential equation (7). We thus can view the brickwall unitary circuit as a Trotter discretization scheme of the Lindblad Master equation (7).

Quantum Zeno limit corresponds to $\epsilon = 0$ in (A-5), (A-6), when the K and F gates are projecting the spins on pure states $|\downarrow\rangle$ and $|\uparrow\rangle$ respectively, i.e. $K[\cdot], F[\cdot]$ become the so-called reset gates:

$$\sum_{j=1}^2 F_j(0) \rho_{N+1} F_j(0)^\dagger = |\uparrow\rangle\langle\uparrow|, \quad \rho_{N+1} = \text{tr}_{0,1,\dots,N} \rho \quad (\text{A-12})$$

$$\sum_{j=1}^2 K_j(0) \rho_0 K_j(0)^\dagger = |\downarrow\rangle\langle\downarrow|, \quad \rho_0 = \text{tr}_{1,\dots,N,N+1} \rho. \quad (\text{A-13})$$

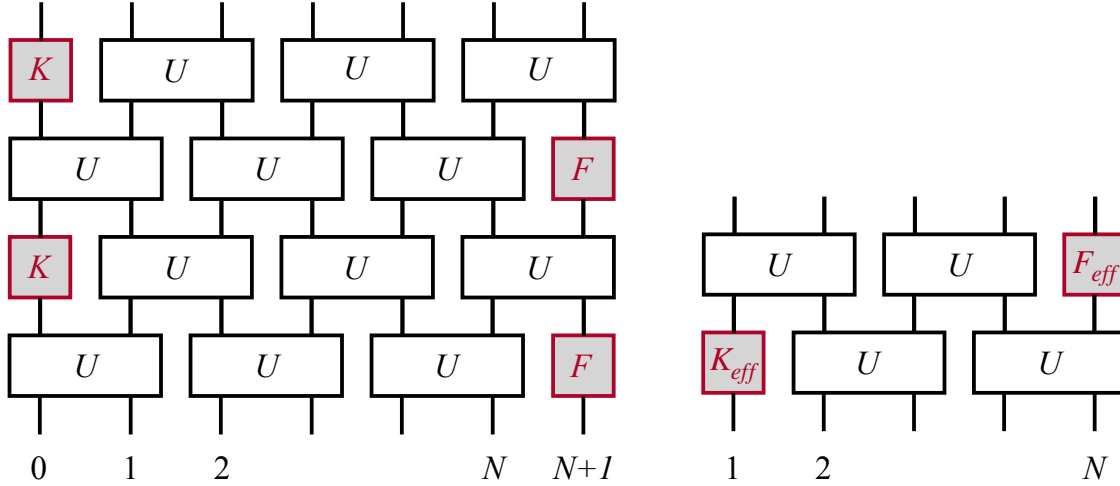


Fig. A-1. Brickwall unitary circuit (BUC), original (left) and effective (right). Left panel shows original BUC with reset gates K and F at the edges. Two-body interaction U is given by (A-4). Right Panel shows effective BUC, where the first site and the last site are traced out, giving rise to effective Krauss operators K_{eff} and F_{eff} .

Indeed, an application of the K and F gates each elementary time step τ can be viewed as an effective realization of a protocol of repeated interactions, leading to quantum Zeno regime. As a result, the quantum chain splits effectively in three parts: spin “0” (always in the state $|\downarrow\rangle\langle\downarrow|$) + internal spins “1, 2, ..., N ” + spin “ $N+1$ ” (always in the state $|\uparrow\rangle\langle\uparrow|$). The bulk interaction affecting the internal spins 1, 2, ..., N gets renormalized, resulting in the application of the effective single spin boundary channels:

$$K_{\text{eff}}(\rho) = \text{tr}_1 \left(U_{12} (|\downarrow\rangle\langle\downarrow| \otimes \rho) U_{12}^\dagger \right), \quad (\text{A-14})$$

$$F_{\text{eff}}(\rho) = \text{tr}_2 \left(U_{12} (\rho \otimes |\uparrow\rangle\langle\uparrow|) U_{12}^\dagger \right), \quad (\text{A-15})$$

acting on spins 1, N , respectively: see Fig. A-1, lower Panel. It can be shown (to be reported elsewhere) that the quantum Zeno NESS (the fixed point of the effective time evolution of the brickwall circuit for $\tau \rightarrow 0$) commutes with the effective Hamiltonian (22).

The above scheme is straightforwardly extendable on all other cases considered in our manuscript.

Appendix B: Numerical evidence showing consistency of Eq. (36)

For cases when $M > 1$, we currently lack full analytic proof of the (36). Nevertheless, this equation can be verified numerically for $M = 2$ and larger M . The ratio ν_β/ν_α obtained from Eq. (36) consistently matches other approaches. Some explicit examples are shown in Tables 1 and 2, for $M = 2$ and $M = 3$, where we employ the following BAE equivalent to Eq. (34)

$$e^{2i(N+1)p_j} \left[\frac{\Delta - e^{ip_j}}{1 - \Delta e^{ip_j}} \right]^2 = \prod_{\sigma=\pm} \prod_{k \neq j}^M \frac{1 - 2\Delta e^{ip_j} + e^{ip_j} e^{i\sigma p_k}}{1 - 2\Delta e^{i\sigma p_k} + e^{ip_j} e^{i\sigma p_k}}, \quad j = 1, \dots, M, \quad (\text{A-1})$$

and $\epsilon(p) = 4(\cos p - \Delta)$.

Appendix C: Numerical evidence showing consistency of Eq. (43)

For XYZ model, we are able to guess the analytic expression for the dissipatively dressed dispersion (43). Some technical details followed by an explicit examples are given below.

$p_1^{(\alpha)}$	$p_2^{(\alpha)}$	E	$\log(\nu_\alpha/\nu_1)$
2.6041	2.0574	-6.6398	0
1.5086	2.6122	-4.5374	0.8315
1.5169	2.0803	-3.0687	1.2440
0.9512	2.6300	-2.4983	2.2403
0.4126	2.6596	-1.2134	4.4264
2.1192	0.9537	-1.1040	2.6273
0.4052	2.1843	0.0399	4.8052
0.9620	1.6082	0.8043	3.3183
1.7257	0.3885	1.7515	5.4714
1.2864+0.8655 <i>i</i>	1.2864-0.8655 <i>i</i>	1.8059	1.5936
1.0386+0.2488 <i>i</i>	1.0386-0.2488 <i>i</i>	2.8522	4.2450
0.3566	1.2991	3.4884	6.4596
0.7405	0.8791	4.1706	5.9499
0.9129	0.3134	4.9178	7.7571
0.2771	0.5625	5.8978	9.2974

Tab. 1. Numerical solutions of BAE (A-1) and the entanglement NESS spectrum. Here $N = 5, M = 2$ and $\Delta = \frac{2}{3}$.

Define the following state

$$|\Psi(n_1, \dots, n_M)\rangle = \bigotimes_{l_1=1}^{n_1} \psi(l_1) \bigotimes_{l_2=n_1+1}^{n_2} \psi(l_2-2) \cdots \bigotimes_{l_{M+1}=n_M+1}^N \psi(l_{M+1}-2M), \quad (\text{A-1})$$

$$\psi(x) = \begin{pmatrix} \bar{\theta}_1(\varepsilon + x\eta) \\ -\bar{\theta}_4(\varepsilon + x\eta) \end{pmatrix}, \quad \varepsilon = u_l = x_l + iy_l. \quad (\text{A-2})$$

Similarly to the XXZ case with XY plane boundary targeting, the set

$$|\Psi(n_1, \dots, n_M)\rangle, \quad 0 \leq n_1 < n_2 \cdots < n_M \leq N,$$

forms a chiral invariant subspace of

$$H_D = \sum_{n=1}^{N-1} \vec{\sigma}_n \hat{J} \vec{\sigma}_{n+1} + h_1(\vec{n}_l) + h_N(\vec{n}_r), \quad (\text{A-3})$$

if special values of \vec{n}_l, \vec{n}_r are chosen, see Eq. (38) in the main text.

One can use the chiral states (A-1) to expand the Bethe state inside the invariant subspace and the corresponding expansion coefficients depend on the Bethe roots $\{u_1, \dots, u_M\}$ in (39) [19].

Under the dynamics of the XYZ Hamiltonian, the Zeno NESS has reduced rank $d_M = \binom{N+1}{M}$, namely,

$$\rho_{\text{NESS}} = \sum_{\alpha=1}^{d_M} \nu_\alpha |\alpha\rangle \langle \alpha|. \quad (\text{A-4})$$

where $|\alpha\rangle$ are eigenstates of H_D (A-3) belonging to the chiral invariant subspace.

The operators $g_{l,r}$ can be written in terms of elliptic functions as follows:

$$g_l = G_L \otimes I^{\otimes N-1}, \quad g_r = I^{\otimes N-1} \otimes G_R,$$

$$G_{L,R} = \begin{pmatrix} \frac{\theta_2(\eta)\sqrt{\theta_1(x_{l,r}-iy_{l,r})\theta_1(x_{l,r}+iy_{l,r})}}{\theta_4(x_{l,r})\theta_3(iy_{l,r})} & -\frac{\theta_1(x_{l,r}-iy_{l,r})[\theta_4(\eta)\theta_3(x_{l,r}+iy_{l,r})-\theta_3(\eta)\theta_4(x_{l,r}+iy_{l,r})]}{\theta_4(x_{l,r})\theta_3(iy_{l,r})\sqrt{\theta_1(x_{l,r}-iy_{l,r})\theta_1(x_{l,r}+iy_{l,r})}} \\ -\frac{\theta_1(x_{l,r}-iy_{l,r})[\theta_3(\eta)\theta_4(x_{l,r}+iy_{l,r})+\theta_4(\eta)\theta_3(x_{l,r}+iy_{l,r})]}{\theta_4(x_{l,r})\theta_3(iy_{l,r})\sqrt{\theta_1(x_{l,r}-iy_{l,r})\theta_1(x_{l,r}+iy_{l,r})}} & -\frac{\theta_2(\eta)\sqrt{\theta_1(x_{l,r}-iy_{l,r})\theta_1(x_{l,r}+iy_{l,r})}}{\theta_4(x_{l,r})\theta_3(iy_{l,r})} \end{pmatrix}. \quad (\text{A-5})$$

$p_1^{(\alpha)}$	$p_2^{(\alpha)}$	$p_3^{(\alpha)}$	E	$\log(\nu_\alpha/\nu_1)$
2.1710	2.6609	1.6539	-9.4713	0
1.1143	2.1955	2.6721	-7.4769	1.1630
2.2510	0.5090	3.5861	-5.9674	3.3356
1.7101	1.1263	2.676	-5.7429	1.7502
2.2068	1.7148	1.1306	-4.5789	2.0594
2.7009	1.8138	0.4928	-4.3896	3.9236
2.6694	$1.2008+0.6111i$	$1.2008-0.6111i$	-3.4460	1.7685
2.2621	0.4860	1.8187	-3.3285	4.2366
0.4550	1.3969	2.7080	-2.6780	4.8481
2.1861	$1.2128-0.6428i$	$1.2128+0.6428i$	-2.2398	1.9781
3.5856	$0.9363-0.1577i$	$0.9363+0.1577i$	-2.1442	4.0653
1.4017	2.2764	0.4486	-1.6501	5.1467
0.3894	1.0133	3.5639	-1.1651	6.1495
2.2529	$0.9381-0.1605i$	$0.9381+0.1605i$	-1.0633	4.3462
1.6596	$1.2492-0.7461i$	$1.2492+0.7461i$	-0.4221	2.2348
0.3843	1.0153	2.2998	-0.1800	6.4309
0.4343	1.8503	1.4124	-0.1772	5.6766
2.7341	0.6441	0.3290	-0.0218	7.7711
1.8046	$0.9432+0.1685i$	$0.9432-0.1685i$	0.5048	4.8354
0.3250	0.6419	2.3311	0.9047	8.0426
1.0197	1.8869	0.3738	1.2413	6.9218
1.0909	$1.3074-0.9403i$	$1.3074+0.9403i$	1.5866	2.6908
1.9386	0.3170	0.6368	2.2449	8.5127
1.3068	$0.9753-0.2139i$	$0.9753+0.2139i$	2.3009	5.5199
6.6372	1.4846	1.0309	2.8193	7.6528
0.5572	$1.3522+1.1229i$	$1.3522-1.1229i$	3.0105	3.8879
0.4728	$1.1858-0.5741i$	$1.1858+0.5741i$	3.7407	6.5804
0.3033	0.6254	1.5671	3.7418	9.2056
1.4664	$0.6801+0.4587i$	$0.6801-0.4587i$	3.9690	6.6551
0.3363	$1.0639-0.3143i$	$1.0639+0.3143i$	4.5199	8.4020
0.6724	$0.8847-0.0706i$	$0.8847+0.0706i$	4.8769	8.2448
0.5961	1.2358	0.2830	5.1327	10.1424
0.2880	$0.9049-0.1041i$	$0.9049+0.1041i$	5.4709	9.8548
0.2598	0.9604	0.5368	6.2627	11.2949
0.4815	0.7035	0.2388	7.1487	12.5699

Tab. 2. Numerical solutions of BAE (A-1) and the entanglement NESS spectrum. Here $N = 6$, $M = 3$, and $\Delta = \frac{2}{3}$.

Similarly to the XXZ case, one can prove that all chiral states $|\Psi(n_1, \dots, n_M)\rangle$ are eigenstates of g_l and g_r :

$$g_l |\Psi(s, n, m, \dots)\rangle = (1 - 2\delta_{s,0})\kappa_l |\Psi(s, n, m, \dots)\rangle, \quad (\text{A-6})$$

$$g_r |\Psi(n, m, \dots, s)\rangle = (2\delta_{s,N} - 1)\kappa_r |\Psi(n, m, \dots, s)\rangle, \quad (\text{A-7})$$

$$\kappa_{l,r} = \frac{\sqrt{\theta_1(x_{l,r} - iy_{l,r})}}{\sqrt{\theta_1(x_{l,r} + iy_{l,r})}} \frac{\theta_1(\eta)\theta_2(x_{l,r} + iy_{l,r})}{\theta_4(x_{l,r})\theta_3(iy_{l,r})}. \quad (\text{A-8})$$

Define the function

$$Q(x, \{y_k\}) = \prod_{k=1}^M \theta_1(x - y_k + \frac{\eta}{2})\theta_1(x + y_k + \frac{\eta}{2}). \quad (\text{A-9})$$

Hypothesis 1. The spectrum ν_α of the Zeno NESS (A-4) is given by

$$\frac{\nu_\beta}{\nu_\alpha} = \left| \frac{Q(\frac{1-\tau}{2} + iy_l, \{u_k^{(\alpha)}\}) Q(0, \{u_k^{(\beta)}\})}{Q(0, \{u_k^{(\alpha)}\}) Q(\frac{1-\tau}{2} + iy_l, \{u_k^{(\beta)}\})} \right|^2, \quad (\text{A-10})$$

where $\{u_j^{(\alpha)}\}$ and $\{u_j^{(\beta)}\}$ are the Bethe roots corresponding to $|\alpha\rangle$ and $|\beta\rangle$ respectively.

Analytic calculations for the XYZ model are extremely complicated due to the involvement of elliptic functions. Therefore, we resort to numerical calculations to verify our hypothesis.

Based on numerical results for the case $M = 1$, we find the following simple and elegant expression:

$$\frac{\nu_\beta}{\nu_\alpha} = \frac{w_{\alpha\beta}}{w_{\beta\alpha}} = \left| \frac{Q(b, u^{(\alpha)})}{Q(a, u^{(\alpha)})} \frac{Q(a, u^{(\beta)})}{Q(b, u^{(\beta)})} \right|^2. \quad (\text{A-11})$$

where a and b are two fixed system-dependent parameters. Some numerical data for the values of a and b is

τ	η	x_l	y_l	a	b
$0.35i$	0.47	0.16	0.05	0	$0.5 - 0.125i$
$0.35i$	0.47	0.71	0.05	0	$0.5 - 0.125i$
$0.35i$	0.47	0.16	0.67	0	$0.5 + 0.495i$
$0.35i$	0.47	0.16	0.49	0	$0.5 + 0.315i$
$0.35i$	0.47	0.16	0	0	$0.5 - 0.175i$
$0.35i$	0.55	0.16	0.05	0	$0.5 - 0.125i$
$0.49i$	0.47	0.16	0.75	0	$0.5 + 0.505i$

On the base of numerics we conclude that

$$a = 0, \quad b = \frac{1 - \tau}{2} + iy_l.$$

For larger M , numerical results (see e.g. Tabs. 3 and 4 for an illustration) also indicate that

$$\frac{\nu_\beta}{\nu_\alpha} = \frac{w_{\alpha\beta}}{w_{\beta\alpha}} = \left| \frac{Q(\frac{1-\tau}{2} + iy_l, \{u_k^{(\alpha)}\}) Q(0, \{u_k^{(\beta)}\})}{Q(0, \{u_k^{(\alpha)}\}) Q(\frac{1-\tau}{2} + iy_l, \{u_k^{(\beta)}\})} \right|^2, \quad (\text{A-13})$$

where Q is given by Eq. (A-9). Equation (A-10) notably results in the dressed energy given by Eq. (43).

When $\tau \rightarrow +i\infty$, the XYZ model reduces to the XXZ model with $\{J_x, J_y, J_z\} \rightarrow \{1, 1, \cos(\pi\eta)\}$. By letting $iy_{l,r} = \frac{\tau}{2}$ and $\tau \rightarrow +i\infty$, the targeted boundary polarizations become

$$\begin{aligned} n_{l,r}^x &= -\frac{\theta_2(\frac{\tau}{2}) \theta_1(x_{l,r})}{\theta_3(\frac{\tau}{2}) \theta_4(x_{l,r})} = -\sin(\pi x_{l,r}), \\ n_{l,r}^y &= -i \frac{\theta_1(\frac{\tau}{2})}{\theta_3(\frac{\tau}{2})} \frac{\theta_2(x_{l,r})}{\theta_4(x_{l,r})} = \cos(\pi x_{l,r}), \\ n_{l,r}^z &= -\frac{\theta_4(\frac{\tau}{2})}{\theta_3(\frac{\tau}{2})} \frac{\theta_3(x_{l,r})}{\theta_4(x_{l,r})} = 0. \end{aligned} \quad (\text{A-14})$$

The corresponding BAE (39) reduce to the trigonometric ones [17, 22, 23]

$$\begin{aligned} &\left[\frac{\sin(\pi u_j + \frac{\pi\eta}{2})}{\sin(\pi u_j - \frac{\pi\eta}{2})} \right]^{2N+2} \left[\frac{\cos(\pi u_j - \frac{\pi\eta}{2})}{\cos(\pi u_j + \frac{\pi\eta}{2})} \right]^2 \\ &= \prod_{\sigma=\pm 1} \prod_{k \neq j}^M \frac{\sin(\pi u_j + \sigma\pi u_k + \pi\eta)}{\sin(\pi u_j + \sigma\pi u_k - \pi\eta)}, \quad j = 1, \dots, M. \end{aligned} \quad (\text{A-15})$$

In conclusion, we retrieve the result of the previous section in the limit where $iy_{l,r} = \frac{\tau}{2}$ and $\tau \rightarrow +i\infty$.

$u_1^{(\alpha)}$	$u_2^{(\alpha)}$	E	ν_α/ν_1
$0.0532i$	$0.2393i$	-17.5382	1
$0.0532i$	$0.8950+0.1750i$	-16.0715	1.0877
$0.1106i$	$0.1050+0.1750i$	-15.5292	1.1215
$0.2972i$	$0.3050+0.1750i$	-3.2127	2.3593
$0.1100i$	$0.6950+0.1750i$	-2.6720	2.4323
$0.1050+0.1750i$	$0.3050+0.1750i$	-1.1998	2.6465
$0.3032i$	$0.5000+0.2451i$	0.7863	2.8787
$0.2668i$	$0.5000+0.2638i$	1.2244	2.9460
$0.7650+0.1643i$	$0.7650+0.1857i$	1.2589	3.0816
$0.1192i$	$0.5000+0.0645i$	1.6803	3.0172
$0.1050+0.1750i$	$0.5000+0.1174i$	2.7827	3.2291
$0.5000+0.0581i$	$0.1050+0.1750i$	3.1085	3.2729
$0.5000+0.2359i$	$0.3050+0.1750i$	15.6611	7.0102
$0.5000+0.0559i$	$0.6950+0.1750i$	15.9818	7.1036
$0.5000+0.1141i$	$0.5000+0.2941i$	19.9809	8.6736

Tab. 3. Numerical solutions of BAE (39) and the entanglement NESS spectrum. Here $\eta = 0.47$, $N = 5$, $M = 2$, $\tau = 0.35i$, $\{x_l, y_l\} = \{0.13, 0.21\}$.

$u_1^{(\alpha)}$	$u_2^{(\alpha)}$	$u_3^{(\alpha)}$	E	ν_α/ν_{10}
$0.1050+0.1750i$	$0.1107i$	$0.2967i$	-26.4413	0.3315
$0.0520i$	$0.2412i$	$0.3650+0.1750i$	-11.1247	0.8185
$0.8954+0.1750i$	$0.3651+0.1750i$	$0.0520i$	-9.6473	0.8907
$0.6351+0.1750i$	$0.8946+0.1750i$	$0.2980i$	-9.6357	0.8914
$0.1088i$	$0.1046+0.1750i$	$0.6348+0.1750i$	-9.1113	0.9181
$0.1088i$	$0.6352+0.1750i$	$0.1054+0.1750i$	-9.1005	0.9187
$0.8950+0.1750i$	$0.0470i$	$0.5000+0.1076i$	-8.1303	0.9539
$0.5000+0.0900i$	$0.0846i$	$0.1050+0.1750i$	-7.6879	0.9765
$0.8950+0.1750i$	$0.6594+0.1750i$	$0.1294+0.1750i$	-7.6318	1.0058
$0.5000+0.0664i$	$0.8950+0.1750i$	$0.1194i$	-7.2318	1
$0.5000+0.1037i$	$0.0458i$	$0.3650+0.1750i$	7.2253	2.3593
$0.0819i$	$0.5000+0.2646i$	$0.3650+0.1750i$	7.6562	2.4135
$0.6350+0.1750i$	$0.2350+0.1636i$	$0.7650+0.1636i$	7.6989	2.5260
$0.3650+0.1750i$	$0.5000+0.0636i$	$0.1176i$	8.1122	2.4718
$0.5000+0.1164i$	$0.8952+0.1750i$	$0.3651+0.1750i$	9.2246	2.6469
$0.6351+0.1750i$	$0.1052+0.1750i$	$0.5000+0.1164i$	9.2304	2.6479
$0.6349+0.1750i$	$0.5000+0.0572i$	$0.1048+0.1750i$	9.5490	2.6825
$0.1052+0.1750i$	$0.3649+0.1750i$	$0.5000+0.0572i$	9.5566	2.6838
$0.1050+0.1750i$	$0.5000+0.0572i$	$0.5000+0.1163i$	11.0593	2.8735
$0.5000+0.1130i$	$0.5000+0.0551i$	$0.3650+0.1750i$	26.4301	7.1123

Tab. 4. Numerical solutions of BAE (39) and the entanglement NESS spectrum. Here $\eta = 0.47$, $N = 5$, $M = 3$, $\tau = 0.35i$, $\{x_l, y_l\} = \{0.13, 0.21\}$.